

A SQUID Microscope Using a Hollow-Structured Cryostat for Scanning Room-Temperature Rock Samples

Jun Kawai, Masakazu Miyamoto, Hisanao Ogata
Applied Electronics Laboratory
Kanazawa Institute of Technology
Kanazawa, Japan
j-kawai@neptune.kanazawa-it.ac.jp

Hirokuni Oda, Isoji Miyagi, Masahiko Sato
Geological Survey of Japan
National Institute of Advanced Industrial Science
Technology
Tsukuba, Japan

Junichi Fujihira
FEDLIC Co., Ltd.
Tsukuba, Japan

Abstract—We developed a high-resolution superconducting quantum interference device (SQUID) microscope, which employs a hollow cryostat, for magnetic field imaging of rock samples at room temperature. A directly coupled low-temperature SQUID with a $0.2 \times 0.2 \text{ mm}^2$ pick-up loop, mounted on a sapphire conical rod, is separated from a sample at room temperature through a vacuum gap and a 40-micrometer-thick sapphire window. Precise and repeatable adjustment of the vacuum gap is performed by rotating a micrometer spindle connected to the sapphire rod through the hollow of the cryostat. We have achieved the separation of 0.23 mm between the SQUID and a sample. We also demonstrated imaging of the magnetic field of a zircon crystal having magnetite grains.

Keywords—SQUID microscope; magnetic imaging; geological sample

I. INTRODUCTION

Superconducting quantum interference device (SQUID) microscopy for room-temperature samples is a very useful technique to image weak magnetic field distributions with high spatial resolution in the order of $100 \mu\text{m}$ [1-4].

Geological studies such as paleomagnetism and planetary science are one of the interesting applications of this technique [4-9]. In a recent work, a SQUID microscope played an important role in magnetostratigraphic dating as a powerful tool to image fine magnetic stripes related to geomagnetic reversals preserved in rock samples [10].

The SQUID chip in a SQUID microscope is separated from a room-temperature sample through a vacuum gap and a thin non-magnetic window. It is required that the SQUID chip should be as close as possible to the sample in order to obtain not only a good signal-to-noise ratio but also high spatial resolution. Precise adjustment of the vacuum gap with respect

to the sample is essential.

In practical use of a SQUID microscope, users often warm up the system. In this case, the SQUID chip must be sufficiently separated from the window before warming up so that it does not touch and break the thin window because of thermal extension of the cryogenic components. Therefore, the SQUID microscope requires an easy, reliable and repeatable mechanism to adjust the vacuum gap.

In this study, we designed and developed a SQUID microscope for geological sample imaging, employing a hollow-structured cryostat, which easily allows the precise and repeatable adjustment of the vacuum gap.

II. DESIGN OF SQUID MICROSCOPE

A. Structure of the Cryostat

A photograph of the cryostat and a schematic of its cross section are presented in Fig. 1. The thermal shields and super insulations are not shown in the cross section. The cylindrical vacuum chamber, whose diameter is 370 mm, is made of aluminum except for the bottom. The liquid helium reservoir made of GFRP (glass fiber reinforced plastics) has a hollow through its center. The diameters of the reservoir and the hollow are 240 and 20 mm, respectively. The liquid helium capacity is about 10 liters. The liquid helium supply and gas-exhaustion ports are located symmetrically with respect to the center.

A rigid GFRP shaft is passed through the hollow and connected to a small bellows that is fixed to the top flange of the vacuum chamber. A micrometer spindle is attached to the bellows so that its rotation expands or shrinks the bellows. Thus, the rigid shaft moves up and down by rotating the micrometer spindle at room temperature. The end of the shaft is connected to a copper rod with a flexure spring, which

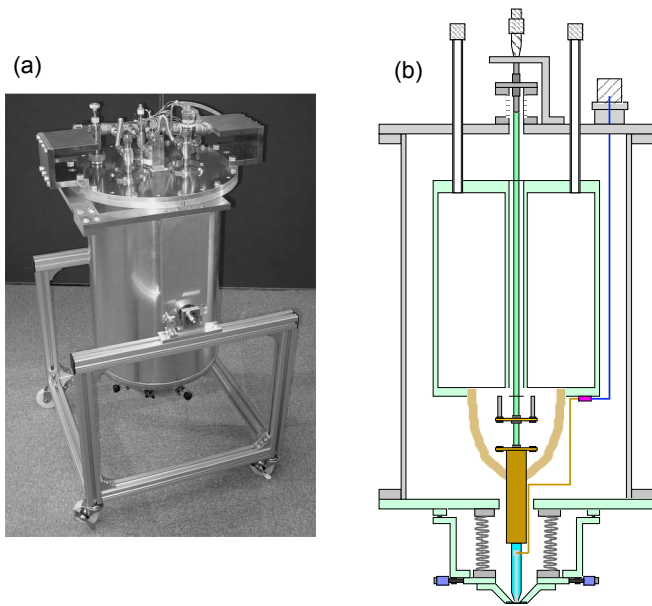


Fig. 1. Photograph of the SQUID microscope (a) and schematic of its cross section (b). The SQUID chip mounted on the sapphire tip is moved up and down by rotating the micrometer spindle on the top.

allows the rod to move only in the vertical direction. The copper rod is thermally anchored to the helium reservoir by copper-wire bundles. A sapphire rod with a SQUID chip mounted on the conical top is tightly connected to the copper rod. Using this mechanism, the vertical movement of the SQUID chip was achieved with an accuracy of $\sim 5 \mu\text{m}$ in the movable range of 1 mm.

The vacuum space is separated from room-temperature environment are separated by a $40\text{-}\mu\text{m}$ thick sapphire window with 3 mm in diameter. We estimate the bowing of the window due to the atmospheric pressure to be $\sim 10 \mu\text{m}$ [11]. The sapphire window is supported by a thicker sapphire-backing plate attached to a GFRP cone, and the cone is connected to an aluminum bellows, which is attached to the bottom of the vacuum chamber. By moving the bellows using vertical and horizontal screws, we roughly position the SQUID chip with respect to the sapphire window before

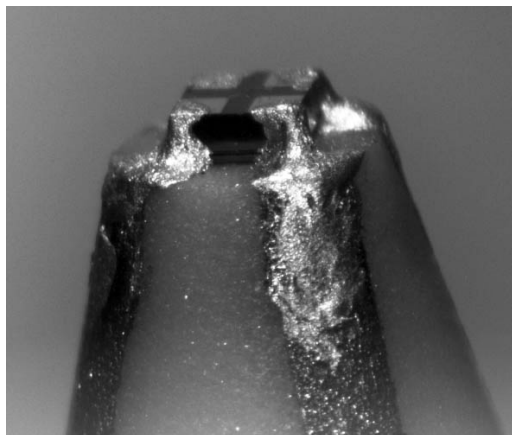


Fig. 2 SQUID chip mounted on the sapphire tip.

making precise adjustments using the micrometer spindle.

B. SQUID and Assembly

The SQUID is a simple washer-type magnetometer fabricated on a $1 \times 1 \text{ mm}^2$ silicon substrate using a Nb/AlOx/Nb-based process. The sizes of the SQUID washer and the hole are $200 \times 200 \mu\text{m}^2$ and $30 \times 30 \mu\text{m}^2$, respectively. The maximum voltage output was $76 \mu\text{V}$ in a superconductive shielding in liquid helium.

This SQUID chip was glued on the tip of the sapphire rod and electrically connected to silver-based thin-film electrodes using silver paste. The silver-based thin-film electrodes were metalized on the surface of the sapphire rod from the bottom to the conical top in advance. Fig. 2 is a photograph of the SQUID chip mounted on the sapphire tip. The diameter of the tip is 2 mm.

Electrical wiring from the sapphire rod to room-temperature electronics passes through the vacuum layer of the cryostat. Copper wires, soldered to the electrodes at the bottom of the sapphire rod, were connected to highly-resistive wires via an RC filter to eliminate high-frequency interference. The highly-resistive wires were terminated at the connectors on the top flange of the liquid helium reservoir.

C. Low-Drift Flux-Locked Loop

While scanning a rock sample with the SQUID microscope, low-frequency drift noise in the output signal should be eliminated because high-spatial-resolution scanning takes hours. In flux-locked loop operation of low-temperature SQUIDs, the low-frequency drift noise is mainly attributed to the temperature change of the preamplifier. We developed a low-drift FLL with direct voltage readout in combination with switching and sample hold functions in order to eliminate the low-frequency drift noise.

Fig. 3 is an equivalent circuit of the low-drift FLL with voltage readout. The bias current applied to the SQUID switches on and off at 20 kHz. The output from the preamplifier also switches to two circuits with the same timing. When the bias is off, the signal is output through the upper circuit (A) in Fig. 3, where only the drift noise is sampled and held. While the bias is on, the measurement signal including the drift noise is sampled and held through the circuit (B). By subtracting the signal measured through (A) from the signal measured through (B) in front of the integrator, we eliminate the low-frequency drift in the measurement signals.

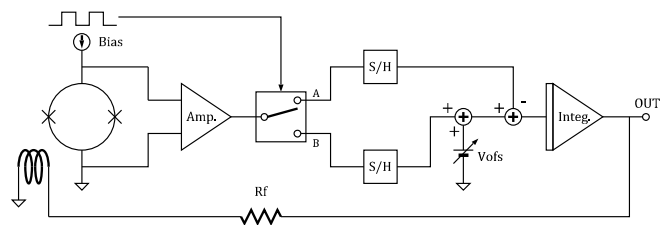


Fig. 3. Equivalent circuit of the low-drift FLL with voltage readout.

D. Performance

When the SQUID microscope was cooled with liquid helium, the temperature of the sapphire rod reached 4.8 K. The maximum output voltage of the SQUID was $67 \mu\text{V}$, which was 15 % smaller than that observed in liquid helium. When the SQUID was operated with the low-drift FLL, we obtained the field noise of $1.1 \text{ pT}/\sqrt{\text{Hz}}$ at 1 Hz in a superconductive shielding. We also confirmed that the low frequency drift due to temperature change was $\sim 10 \text{ pT}/^\circ\text{C}$.

The separation between the SQUID and the sapphire window was estimated by scanning the magnetic field generated with a 1-mA DC line current, which was applied to a 25- μm -thick and 100-mm-long aluminum wire. We have achieved the separation between the SQUID and the wire of 230 μm . We evaluated the precision of the adjustment of the separation between the SQUID and the sapphire window, repeating up-and-down movements of the sapphire rod by rotating the micrometer spindle. The difference in the separation among five runs was within $\pm 5 \mu\text{m}$ for a movement of 200 μm .

The boil-off rate of the liquid helium was 3.3 L/day, and stable performance of the SQUID was maintained for almost 3.5 days until the liquid helium reservoir was empty.

III. DEMONSTRATION OF IMAGING

We demonstrated magnetic imaging of a natural zircon crystal using the SQUID microscope. The zircon crystal was about 0.5 mm in size and contained magnetite grains. Isothermal remanent magnetization with a field of 140 mT was artificially imparted to the zircon crystal, resulting in the magnetic moment of $1.9 \times 10^{-10} \text{ Am}^2$. Then, the zircon crystal was buried in the surface of a resin cylinder with 25 mm in diameter and 5 mm in thickness so that the magnetic moment was perpendicular to the surface of the cylinder. The distance between the surface of the resin and the SQUID was set to be about 500 μm . Fig. 4a shows a microscopic picture of the surface of the resin, where the zircon crystal is inside the white dotted circle. By scanning this zircon sample with the SQUID microscope, we obtained an image of a magnetic dipole-like field of $\sim 180 \text{ nT}$ (Fig. 4b), which is consistent with the calculated magnetic field using the magnetic moment of $1.9 \times 10^{-10} \text{ Am}^2$ and the distance of 500 μm . According to this result,

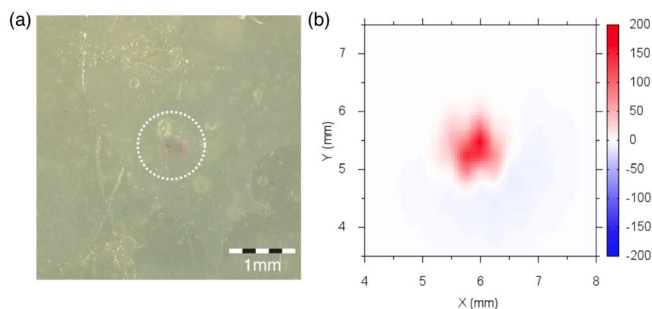


Fig. 4 Microscopic picture of a zircon crystal buried in the surface of a resin (a), and the scanned results (b).

we consider that this SQUID microscope has the sensitivity to image magnetic moments in the order of 10^{-14} Am^2 or smaller.

IV. CONCLUSION

We developed a SQUID microscope employing a hollow-structured cryostat and a low-drift FLL. We confirmed that the SQUID microscope could be applied for the fine magnetic imaging of geological samples.

ACKNOWLEDGMENT

The authors thank Ms. M. Kawabata from Eagle Technology Inc. for fabricating the SQUID chip.

REFERENCES

- [1] J. R. Kirtley and J. P. Wikswo, Jr., "SCANNING SQUID MICROSCOPY," *Annu. Rev. Mater. Sci.*, vol. 29, 1999, pp. 117–148.
- [2] S. Chatrathorn, E. F. Fleet, and F. C. Wellstood, "Scanning SQUID microscopy of integrated circuits," *Appl. Phys. Lett.*, vol. 76, 2000, pp. 2304–2306.
- [3] Y. Ono and A. Ishiyama, "Development of biomagnetic measurement system for mice with high spatial resolution," *Appl. Phys. Lett.*, vol. 85, 2004, pp. 332–334.
- [4] L. E. Fong, J. R. Holtzer, K. K. McBride, E. A. Lima, and F. Baudenbacher, "High-resolution room-temperature sample scanning superconducting quantum interference device microscope configurable for geological and biomagnetic applications," *Rev. Sci. Instrum.*, vol. 76, 053703, 2005, pp. 1–9.
- [5] F. Baudenbacher, N. T. Peters, and J. P. Wikswo, Jr., "High resolution low-temperature superconductivity superconducting quantum interference device microscope for imaging magnetic fields of samples at room temperature," *Rev. Sci. Instrum.*, vol. 73, 2002, pp. 1247–1254.
- [6] F. Baudenbacher, L. E. Fong, and J. R. Holtzer, "Monolithic low-transition-temperature superconducting magnetometers for high resolution imaging magnetic fields of room temperature samples," *Appl. Phys. Lett.*, vol. 82, 2003, pp. 3487–3489.
- [7] B. P. Weiss, J. L. Kirschvink, F. J. Baudenbacher, H. Vali, N. T. Peters, F. A. Macdonald, and J. P. Wikswo, "A Low Temperature Transfer of ALH84001 from Mars to Earth," *Science*, vol. 290, 2000, pp. 791–795.
- [8] B. P. Weiss, E. A. Lima, L. E. Fong, and F. Baudenbacher, "Paleointensity of the Earth's magnetic field using SQUID microscopy," *Earth Planet. Sci. Lett.*, vol. 264, 2007, pp. 61–71.
- [9] Q. Wang, H. Qin, Q. Liu, and T. Song, "Room temperature sample scanning SQUID microscope for imaging the magnetic fields of geological specimens," *Applied Mechanics and Materials*, vol. 475–476, 2014, pp. 3–6.
- [10] H. Oda, A. Usui, I. Miyagi, M. Joshima, B. P. Weiss, C. Shantz, L. E. Fong, K. K. McBride, R. Harder, and F. Baudenbacher, "Ultrafine-scale magnetostratigraphy of marine ferromanganese crust," *Geology*, vol. 39, 2011, pp. 227–230.
- [11] T. S. Lee, E. Dantsker, and J. Clarke, "High-transition temperature superconducting quantum interference device microscope," *Rev. Sci. Instrum.*, vol. 67, 1996, pp. 4208–4215.